Exploring the regeneration potential of salivary glands using organoids as a model

Rocchi, Cecilia

DOI:
10.33612/diss.168896082

CHAPTER 6

A MOLECULAR NETWORK-BASED APPROACH REVEALS HUMAN SALIVARY GLAND STEM CELL FEATURES

Rocchi C., Barazzuol L., Boekhoudt J., Jellema- de Bruin A., Baanstra M., Brouwer U., van Os R., Guryev V., Coppes RP.

In preparation

ABSTRACT

The need to restore functionality of salivary gland after irradiation treatment is still unmet. Tissue regenerative strategies could provide opportunities to treat radiation-induced salivary gland dysfunction. However, the molecular processes driving cell fate specification and regulating the balance between regeneration and differentiation are not completely understood. Here we describe the construction and validation of the first molecular network of human salivary gland-derived organoids. Using RNA sequence data obtained from different organoid culture conditions, aimed at enriching for stem cells or functional secretory salivary gland cells, we first build a molecular network based on modules of co-expressed genes. Next, we relate these modules to stem cell traits. This enabled us to identify novel biological processes and specific genes associated with salivary gland regeneration potential and stem-like cell features such as organoid forming ability and long-term self-renewal.

INTRODUCTION

Salivary glands are crucial for maintaining the health of the oral cavity as well as for enabling vital daily activity such as speaking, eating and swallowing [1-3]. Radiotherapy treatment for head and neck cancer, autoimmune diseases like Sjogren's Syndrome as well as natural ageing, all lead to salivary gland dysfunction through progressive degeneration of the secretory acinar cell compartment of the glands [4]. This results in irreversible loss of saliva production and a life time of dry mouth and co-morbidities that drastically decrease the quality of life of the patients affected[5,6]. Despite decades of research, clinically available treatment options for xerostomia patients are palliative, focused on providing short term relief from the symptoms without providing long-term restoration of the gland [4]. Many strategies, including cell therapy [7,8], *in vivo* reactivation of resident stem/progenitor cells [9], restoration of the niche via for example removal of senescence cells [10] and gene therapy[11,12], have been proposed to restore functionality of damaged salivary glands.

While in several organs the identity of tissue specific regenerative cells is known [13], in salivary gland the search for an adult stem cell source possessing the potential to replace acinar cells lost after damage is still ongoing, limiting the potential of regenerative approaches for salivary gland following radiotherapy (Rocchi et al 2020 Npj regenerative medicine, Accepted).

Experiments employing murine cell lineage tracing have allowed major advances in understanding salivary gland epithelial progenitors. However, there is still considerable debate on the nature of the stem/progenitor cells that contribute to tissue homeostasis as well as the mechanisms of regeneration after damage. One model proposes that bipotent murine embryonic salivary gland stem cells (expressing the cytokeratin marker K5) generate ductal and acinar progenitor cells that are postnatally maintained by lineage restricted progenitors. These express the markers K14, Kit/K5 for the ductal cell compartment and SOX2 for the acinar cell compartment [14]. The other model proposes instead a role of plasticity of the salivary gland epithelium in contributing to the functional acinar unit of the irradiated gland[15,16]. We have shown that murine salivary gland-derived epithelial cells from excretory and intercalated ducts can be isolated, grown and expanded *in vitro* as 3D organoids containing differentiated acinar cells and myoepithelial cells [17,18]. These studies suggest that upon activation of proper signaling ductal cells can be directed to give rise to salivary gland tissue-reassembling structures. Transplantation of submandibular salivary gland organoid-derived cells into locally irradiated salivary gland recipient mice allowed 70% rescue of normal total saliva production compared to control-irradiated non-transplanted mice [7,17,18] showing proof-of-principle that regenerative cell therapy approaches could be used for long-term restoration of the damaged salivary gland.

The proven reliability and *in vitro–in vivo* dual usability of salivary gland-derived organoids revealed the potency also of human salivary gland-derived stem/progenitor cells (hSGSPCs)

in rescuing the hyposalivation phenotype when xeno-transplanted into irradiated salivary glands of immunodeficient mice [2]. Although hSGSPCs can be isolated and kept in culture for a number of passages, their potential clinical application is mainly limited by the lack of knowledge regarding the identity of adult hSGSPCs and by the fact that existing culture conditions provide little to no control over their self-renewal and differentiation abilities. While extensive gene expression profiling studies have contributed to the characterization of several adult tissue stem cells and related pathways in homeostatic and disease, adult salivary gland stem cells have not yet been transcriptionally characterized (Rocchi et al 2020, Npj regenerative medicine, Accepted).

Here, we first describe the development of a long-term culture system for human salivary gland derived organoids as well *in vitro* strategies that allow for enrichment of hSGSPCs and differentiation towards more mature salivary gland organoids.

We next hypothesize that RNA sequencing of human salivary gland organoids, enriched for stem cells or differentiated, would enable us to distinguish genes and pathways associated with self-renewal and differentiation of hSGSPCs. We used a network-based gene-weighting approach that allowed the identification of unique groups of co-expressed genes (modules) that represent cellular processes and can be related to the phenotypes of interest [19]. This enabled us to identify genes and gene networks that are directly associated with human salivary gland stem cell related traits. Our findings provide the first set of human salivary gland-derived organoid transcriptomic data and identify molecular pathways which were previously not known to have a pro-regenerative effect in adult salivary glands, such as the fatty acid oxidation pathway. These findings could potentially open new therapeutic strategies for salivary gland dysfunction.

RESULTS

Optimization of human salivary gland culture system

In an attempt to establish a long term human salivary culture system, we adapted our previously established mouse salivary gland culture condition containing Wnt3a, R-spondin and Y-27632 (here called WRY and fully described in the Methods section) [18]. We isolated human salivary gland-derived cells from human submandibular gland biopsies by mechanic and enzymatic digestion, and after 3 days of enrichment in floating culture single cells were seeded in Matrigel (Figure 1A). Organoid formation efficiency (OFE) of single cells obtained from human salivary gland epithelium-derived spheres and cultured in WRY was higher in early passages (P2) compared to those cultured in enriched media (EM) devoid of Wnt3a, R-spondin and Y-27632. However, within 3-4 weeks both culture conditions lost their self-renewal potential, indicating that neither EM nor WRY media was sufficient to promote long-term maintenance of hSGSPCs (Figure 1B and C). Assuming that growth arrest occurred

because of inadequate culture conditions, we next attempted to optimize the culture conditions to increase both the number of stem cell and self-renewal capacity of the stem cells. This was measured as number of passages achievable, by screening various additional growth factors and small molecule modulators under WRY culture condition.

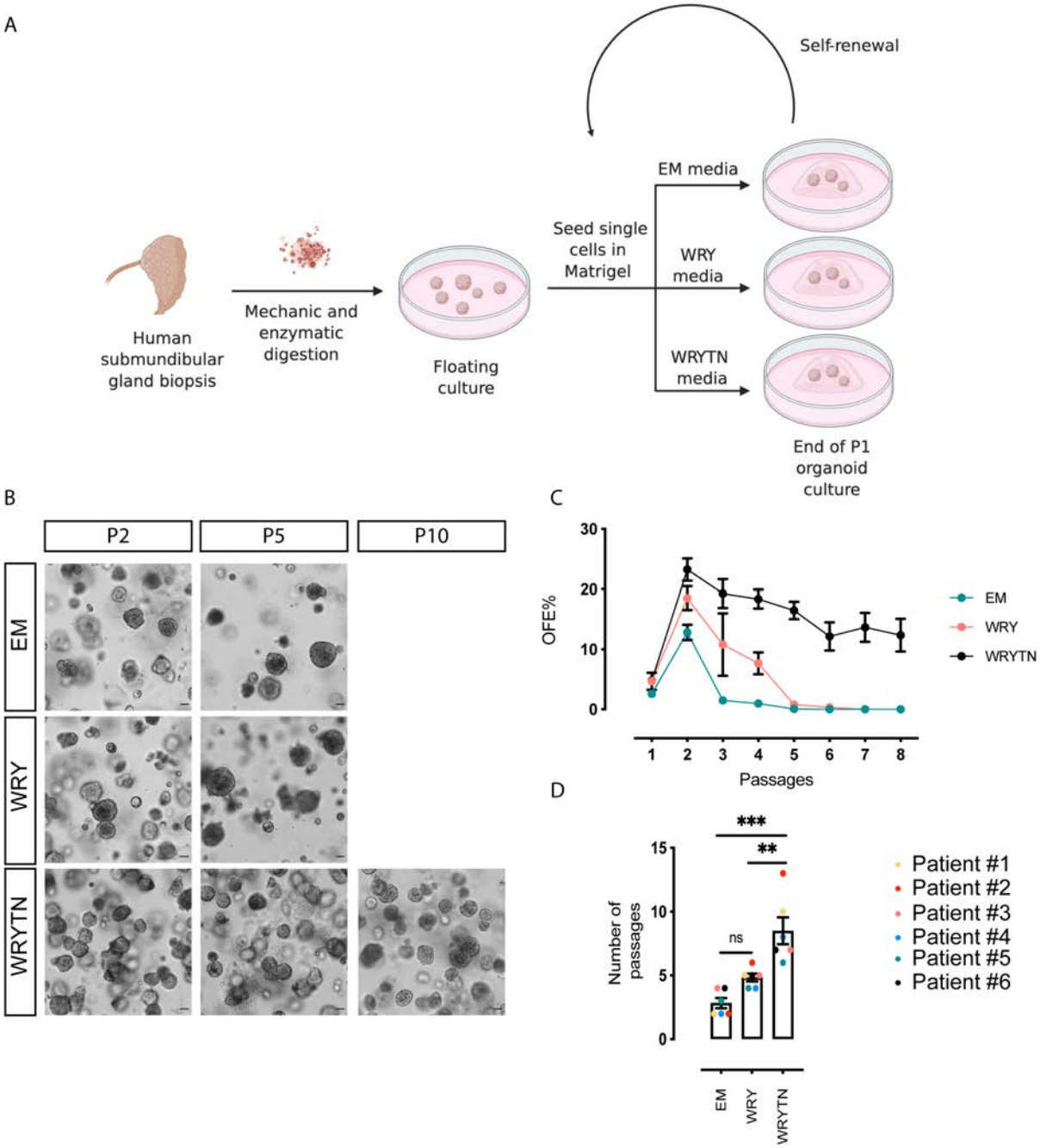

Figure 1: Human-derived submandibular gland organoids can be maintained long-term in culture. A) Schematic representation of the experimental procedure. **B)** Representative brightfield images of human salivary gland-derived organoids grown from single cells seeded in Matrigel® and treated with EM, WRY and WRYTN media at different passages of culture. Scale bar=50 μm **C)** Organoid forming efficiency (OFE) of human-derived salivary gland cells at different passages under the three tested culture conditions (EM, WRY and WRYTN). **D)** Number of passages in culture reached on average under each culture condition. Each color represents a culture

derived from a different patient (n=6). Data are represented as the mean ± SEM (C) and (D). One-way ANOVA (D). *p<0.05, **p<0.01, ***p<0.001, ****p<0.0001.

Although most compounds enhanced self-renewal potential to a certain extent, the combination of two small molecule inhibitors, A83-01 (T; Alk4 inhibitor) and noggin (N; BMP-4 antagonist), synergistically improved both OFE (Figure 1B and C) and long-term culture of hSGSPCs (Supplementary Figure 1B; Figure 1D). This combination allowed culturing up to an average of 8 passages, with a maximum of 12 passages, indicating a maintenance of stem/progenitor cells. Hereafter, we refer to this optimized culture condition as WRYTN.

Combined GSK3B and HDAC inhibition promotes a more primitive and homogeneous salivary gland stem cell organoid culture

In order to obtain a salivary gland stem cell profile in terms of genes and pathways involved in their self-renewal and differentiation, and due to the low yield of stem/progenitor cells in P1, we aimed to further enrich the stem/progenitor cells in subsequent passages. Therefore, we tested the addition of both the GSK3 inhibitor CHIR99021 and the histone deacetylase valproic acid to the WRYTN culture condition. CHIR99021 has previously been shown to promote cell proliferation in epithelial organoids [20,21], while the combination of CHIR99021 and valproic acid promotes Lgr5+ homogeneity in intestinal organoid cultures[22] (Figure 2A). Indeed, also in salivary glands the combined addition of CHIR99021 (3μM) and valproic acid (1mM) (combination now referred to as CV) to the media further enhanced OFE (Figure 2B). To assess whether CV-induced proliferation was due to the enrichment of stem/progenitor cells, we evaluated the potential of treated cells to form secondary and tertiary organoids compared to WRYTN control culture. We observed a significant increase in the ability to form secondary organoids as well as a more active proliferative state of the culture from hSGSPCs that were previously treated with CV compared to untreated WRYTN cultures (Figure 2 B, C, D and E). To further prove that CV treatment leads to a more primitive and undifferentiated stem cell state, we assessed the differentiation potential of CV treated organoids compared to untreated control organoids. To induce differentiation, organoids which had been cultured for 7 days in the presence or absence of CV were re-seeded in Wnt3a-depleted media with the addition of DAPT, an inhibitor of γ-secretase – a key component of the Notch pathway. Removal of Wnt3a and Notch pathway inhibition resulted in clear morphological changes of the organoids derived from the WRYTN control culture conditions (Figure 3B and C), similar to the branching morphogenesis described during embryonic development (Makarenkova et al 2009, Science Signalling). Notably, the continuous presence of CV during differentiation of organoids inhibited changes in organoid morphology, preserved their spherical shape and increased their size, further confirming that CV treatment maintains the cells in a more primitive and

proliferative stem cell state. After withdrawal of CV, organoids regained the ability to differentiate (Figure 3B and C).

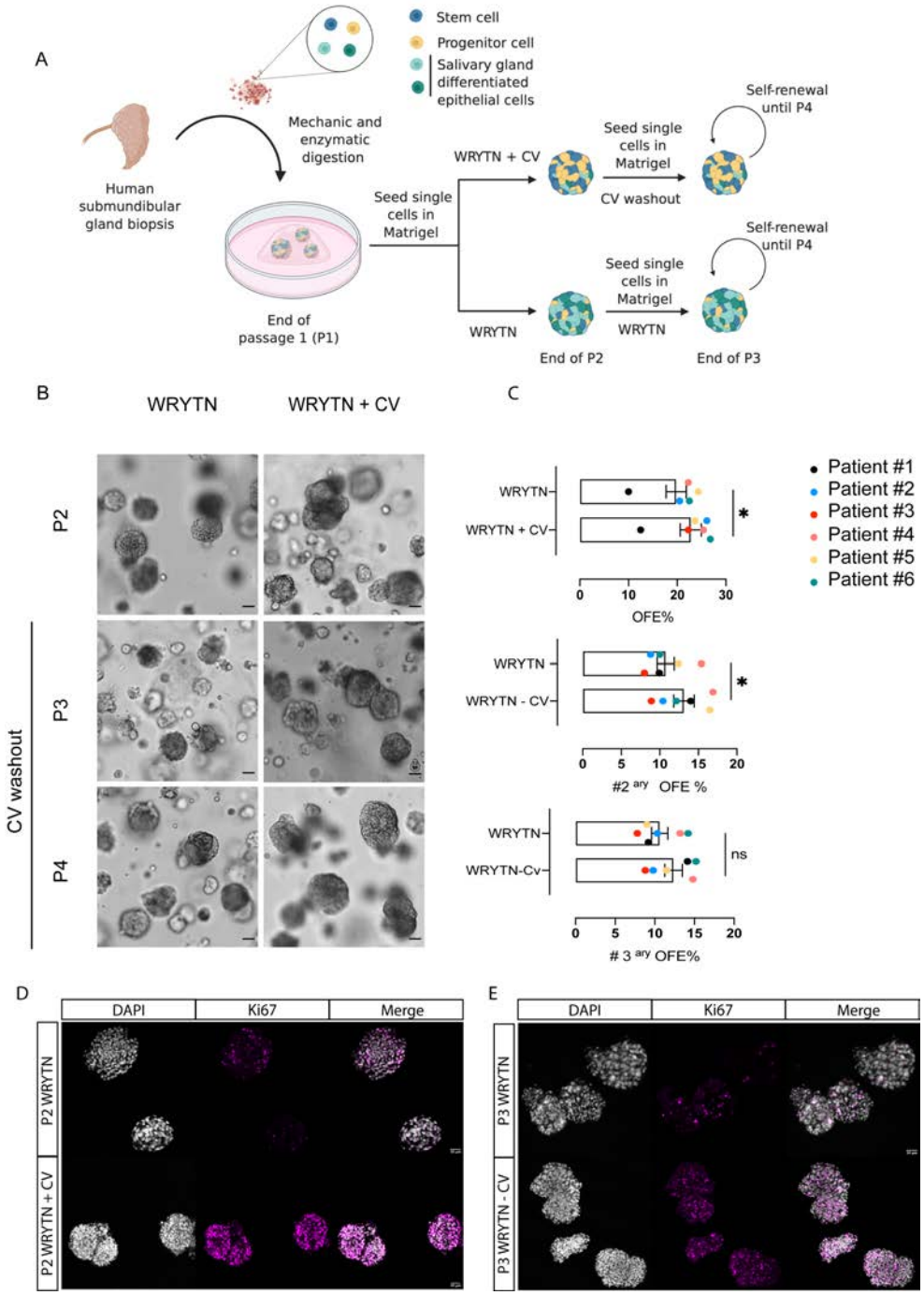

Figure 2: Chir99021 (C) and Valproic Acid (V) treatment increases proliferation and OFE in human salivary gland-derived organoids. A) Schematic drawing of the experimental procedure. Human salivary gland-derived cells were isolated and seeded as single cells in Matrigel®. At the end of the first passage organoids derived from isolated salivary gland-derived cells were trypsinized and re-seeded in Matrigel® and cultured in WRYTN media in presence or absence of CV treatment. At the end of the passage each condition was re-seeded in absence of CV to investigate their ability to form secondary and tertiary organoids. **B)** Representative brightfield images of human salivary gland-derived organoid cultures in WRYTN with or without CV treatment at P2 and after washout (P3 and

P4). Scale bar=50 μm. **C)** Organoid forming efficiency (OFE) of human salivary gland-derived cells at P2 in presence of the treatment, and at P3 and P4 after washout of CV. Each color represents a culture derived from a different patient (n=6). Data are represented as the mean ± SEM (C). One-way ANOVA (C). *p<0.05. **D) and (E)** immunostaining for Dapi (Grey) and ki67 (Magenta) of organoids at P2 and P3. Scale bar=50 μm.

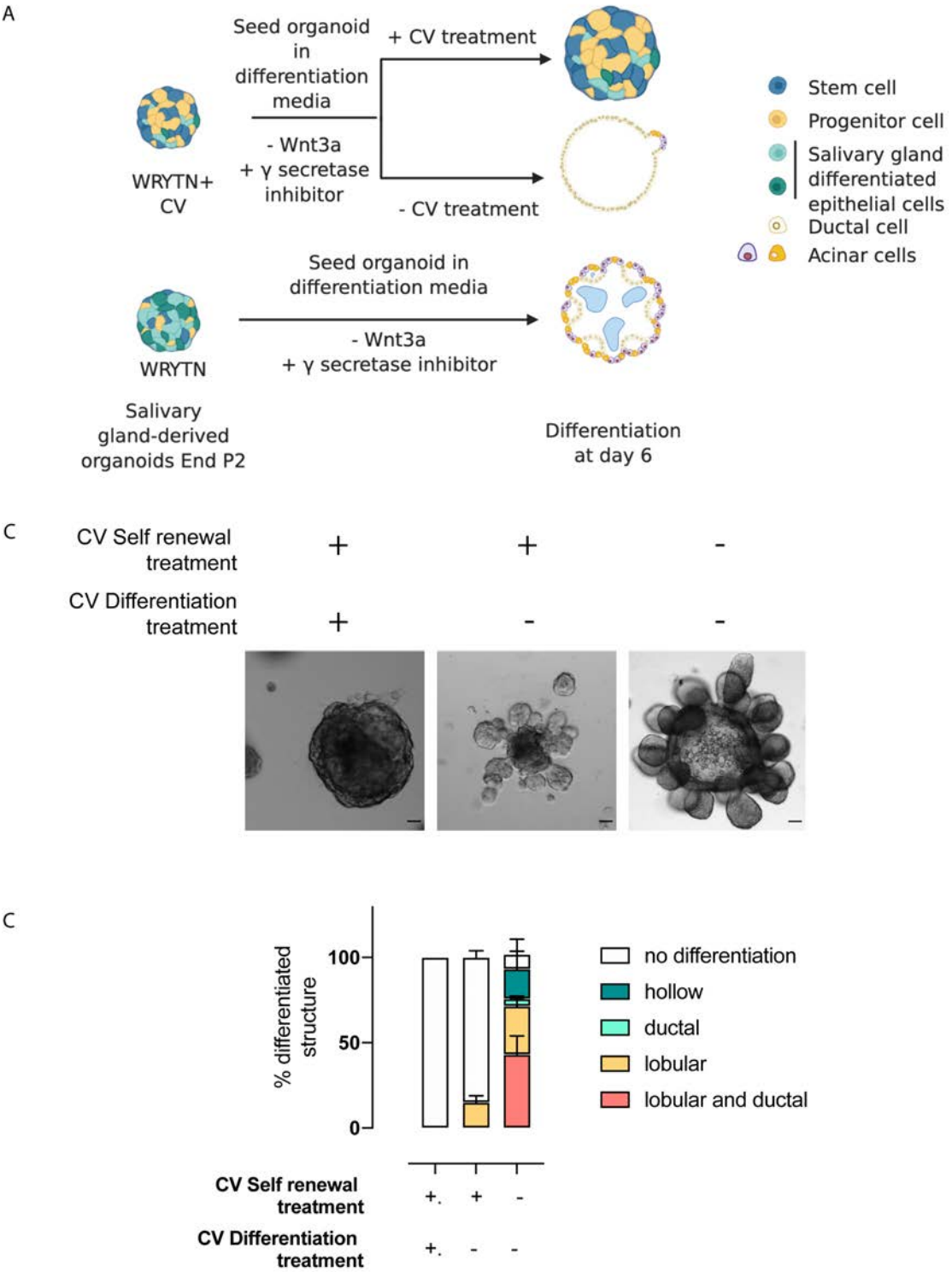

Figure 3: CHIR and Valproic Acid treatment hinders differentiation potential of human salivary gland-derived organoids. A) Schematic representation of the experimental procedure. Organoid cultures in presence or absence of CV treatment at the end of P2 were harvested and seeded in a new gel with and without the CV

treatment in presence of differentiation media. At day 6 of differentiation, the phenotype of the organoids grown from the different conditions were quantified and categorized in different phenotypic category. **B)** Representative brightfield images of human-derived organoids at the end of the differentiation assay. Scale bar=50 μm. **C)** Quantification of the different organoids-phenotypic categories.

These results suggest, in agreement with published data [22,23], that CV treatment of organoids keeps the cells in an undifferentiated state potentially promoting the enrichment for more "primitive" stem/progenitor cells.

Transcriptome analysis of organoids reveals modules of co-expressed genes

To identify a potential signature of hSGSPCs we applied a gene co-expression network analysis (WGCNA) (Zhang B et al, 2005) approach to 10 data sets generated from samples derived from 3 different human salivary gland biopsies (Figure 4A). Six data sets were generated to enable comparison across self-renewal passages of human salivary gland derived organoids cultured in EM and in–WRYTN (at passage P1, P2 and P4). Data set 7 consisted of samples representing human salivary gland-derived organoids enriched in stem cells, which consisted of organoids at P2 cultured in presence of CV (P2 + CV). Data sets 8, 9 and 10 were assembled to compare the differentiation potential of human salivary gland-derived organoids in the presence or absence of CV treatment and after CV withdrawal. Transcriptome profiles of each samples were obtained by [RNA seq methods] and processed for quality control. Principle Component Analysis (PCA) resulted in a consistent segregation of samples (Supplementary Figure 3A) within the different data sets, therefore all samples were included in the analysis. Following data processing, we performed genome-wide gene co-expression analysis [19]. We identified 59 mutually exclusive modules ranging in size between 30 and 700 co-expressed genes hierarchically clustered based on modules eigengenes (MEs) dissimilarity [24] (Figure 4B). Each ME summarizes the characteristic expression pattern of genes that comprise each module. To reveal a consensus transcriptional signature for hSGSPCs, we next assessed the association between each ME and the following phenotypic stem/progenitor cell culture traits: self-renewal and ability to form secondary organoids (OFE), P1 as a more heterogeneous (still unselected) state of the culture and CV treatment as a more primitive (and homogeneous) stem/progenitor cell population. Among the 59 module-trait relationships (Supplementary Figure 3B), three modules (Sienna4, Magenta3 and IndianRed3) showed a positive correlation with OFE and CV treatment indicating that these modules may represent pathways associated with a more primitive stem cell trait, while module Black and Orange, showed a positive correlation with P1 and negative correlations with Sienna4, Magenta3 and IndianRed3 indicating that these modules could represent pathways of a more differentiated trait (Figure 4C).

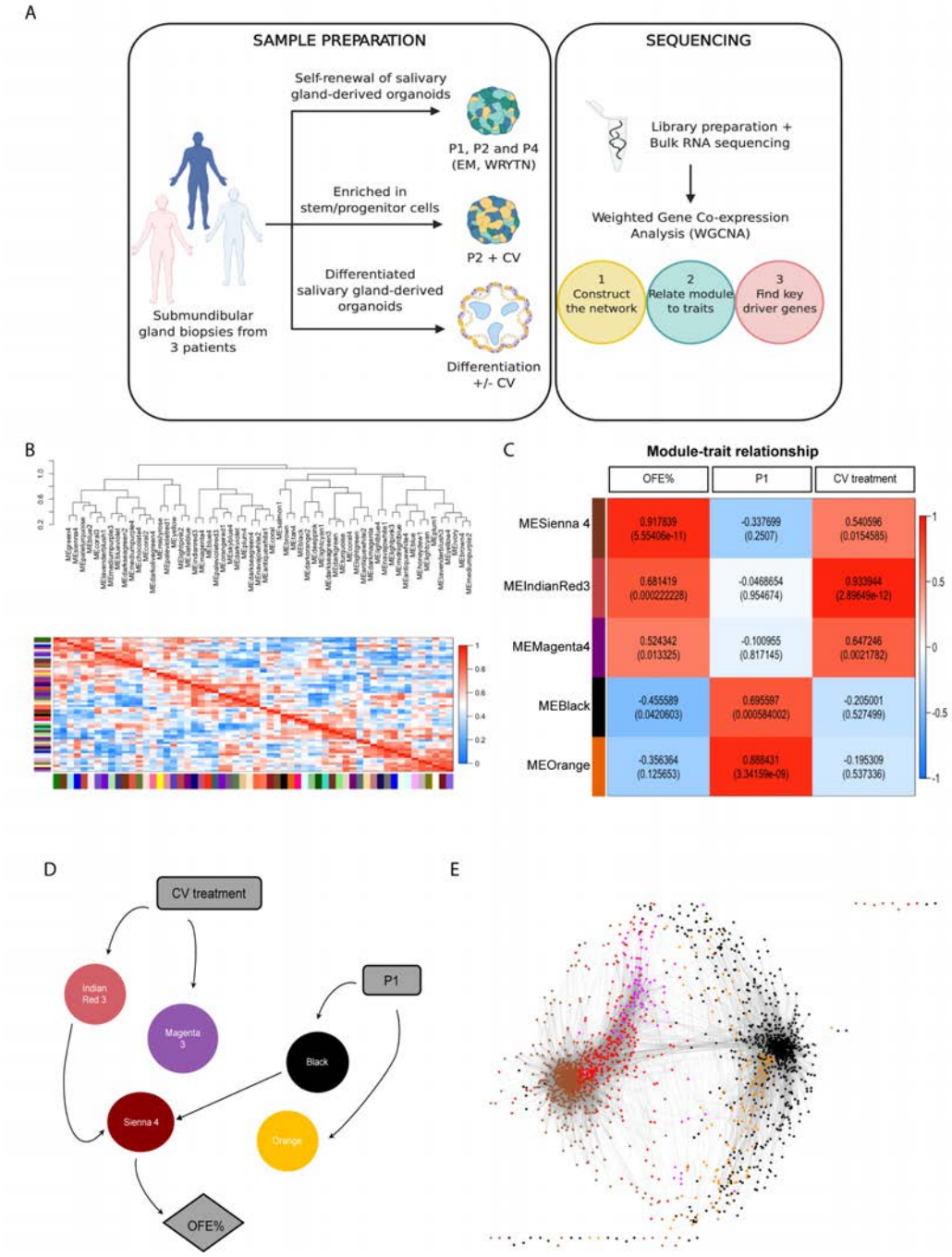

Figure 4: Weighted gene co-expression network analysis of human salivary gland-derived organoids reveals gene co-expression modules. A) Workflow of the strategy used to construct the molecular network. **B)** Structure of the gene co-expression network. Fifty-nine gene co-expression modules were identified and hierarchically cluster based on their module eigengene dissimilarity. **C)** Module-trait association of the module eigengene and culture traits that resemble stem cell features. Each row in the table corresponds to a module and each column to a specific trait. The numbers in the table correspond to the strength of the correlation of the module eigengene and the trait (value= 1 to -1) and the significance of the correlation (P<0.05). The table is colour coded by correlation according to the colour legend. **D)** Directed acyclic graph obtained using Bayesian network structure learning, that represent the relationship between the modules (circles) and the relevant traits (rectangles). **E)** Cytoscape visualization of the complete gene network showing the correlation between each gene within each module and the relation between modules. Each dot represents a gene and each colour represents one of the five

selected modules. The length on the line indicate the strength of the correlation between each gene. The single dots at the top and the bottom of the cytoscape represent genes without any connection in the network.

Subsets of gene co-expression modules correspond to different salivary gland developmental organoid states

We use the intramodular connectivity measure to quantify the similarity between each individual gene within the module and the ME. This is calculated as the Pearson correlation between the expression pattern of a gene and the ME of a module, and quantifies to what extent an individual gene within the module follows the pattern characterized by the ME. This value can be used to identify genes that are the most representative of a module (HUB genes) and that can illustrate a particular cell type or pathway described by that module. In order to understand regulatory loops and dynamic dependency between modules and the stem cell trait, we used a Bayesian network interference approach. A Bayesian network is a probabilistic graphical model where random variables (here being modules and traits) and their conditional dependencies are represented using a directed acyclic graph (DAG)[25]. To limit the network size and focus on more accurate interference, the Bayesian network included: 5 nodes representing trait-associated modules and 3 trait nodes (Figure 4D,E). To determine how the 5 modules (Sienna4, IndianRed3, Magenta3, Orange and Black) represent specific biological processes within salivary gland-derived organoids, we examined the pathway analysis using genes that had a module membership ≥ 0.6 in each module. Module membership indicates how strongly a gene correlates to the module eigengene.

DAVID pathway analysis (https://david.ncifcrf.gov/) revealed a significant enrichment of genes involved in salivary (*P* value = 2.80E-16), pancreatic and gastric secretion indicating a clear glandular transcriptional signature (Figure 5A). This suggests that module Black may represent an acinar progenitor and/or differentiated acinar cells transcriptional signature. Within the 21 genes belonging to the salivary secretion pathway we found mature acinar cells markers, such as *AQP5*, *MUC5B*, *MUC7* and *CHRM3,* as well as defense protein produced by the submandibular gland involved in the innate oral immunity such as Cystatin (*CYS*), and peptide with antimicrobial function such as Histatin (*HIST*). Enzymes, such as lactoperoxidase *(LPO)* or lysozyme *(LYZ)*, are also known to be expressed in adult salivary glands where they contribute to innate salivary gland defense mechanisms[26] (Figure 5B). Interestingly, the cholinergic signaling pathway was one of the pathways most significantly represented in module Black. Cholinergic nerves have been recently reported to play an important role in regulating salivary gland homeostasis and regeneration in adult mouse salivary gland. In mice sublingual gland, cholinergic stimulation acts on Sox2 expressing Chrm3 progenitor cells and activates a Sox2-mediated acinar cell replacement program [9]. Sox2, although not registered

in one of the pathways defined by DAVID, belongs to the module Black with a module membership of 0.6. Taken together these results, particularly the expression profile and high module membership, indicate that the expression signature captured in module Black is specific for acinar cell development. The ability of the cells seeded in P1 to give rise to organoid retaining a secretory profile could indicate that these cells mirror the tissues regeneration process.

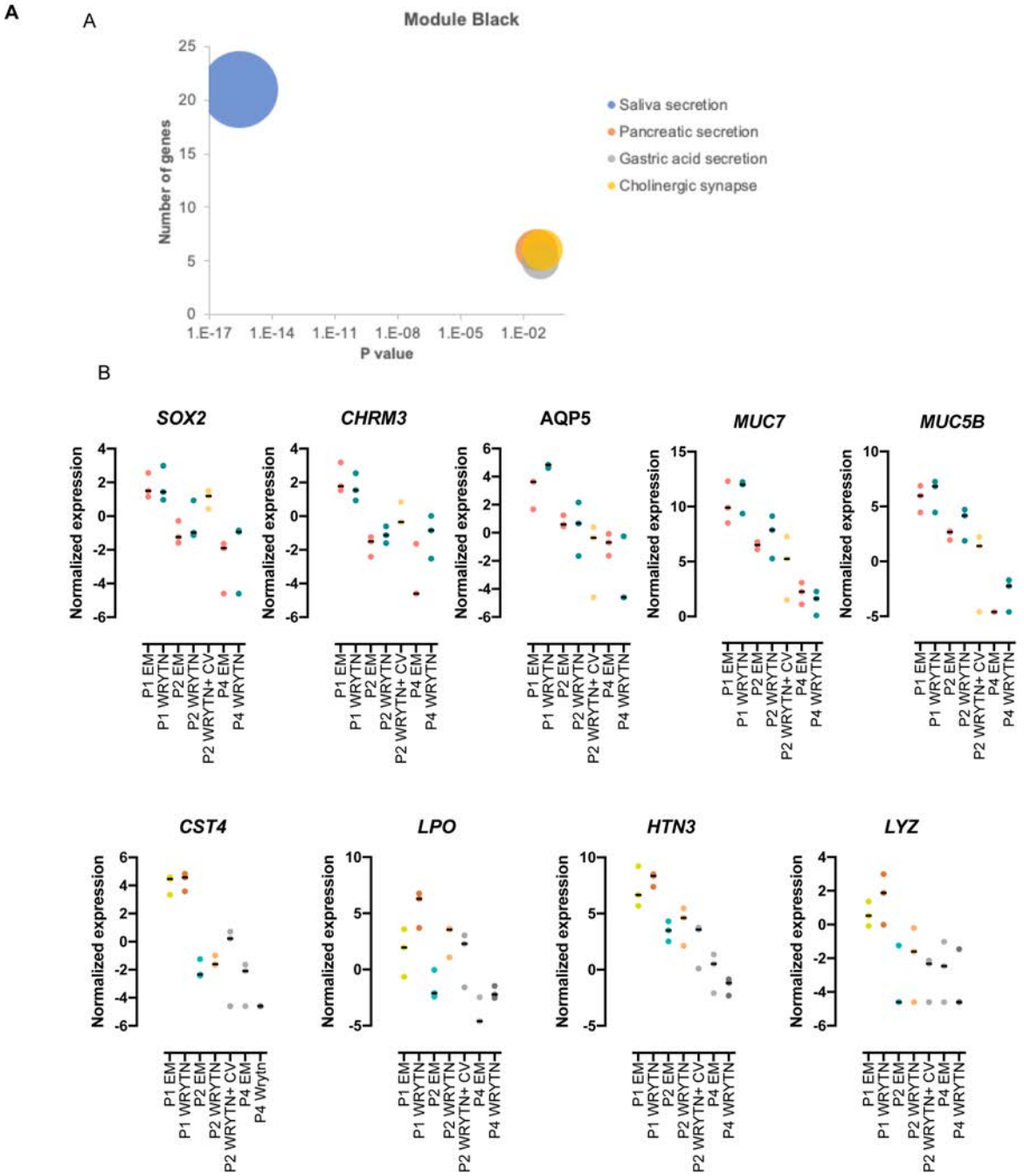

Figure 5: Module Black is representative of acinar development profile. A) Bubble chart representative of the significant pathways obtained by DAVID pathway analysis on MEBlack driver genes (module membership >0,6). Each colour represents a different pathway. The size of the bubble represents the significance of the pathway (P<0.05) and the number of genes enriched in the pathway. **B)** Normalized gene expression of the genes enriched

in the saliva secretion pathway throughout the different culture passages. Each dot represents a single patient. Data are represented as the mean ± SEM.

Module IndianRed describes an enrichment of a pluripotent-like phenotype

The Bayesian network analysis points to IndiaRed3 as the module directly influenced by CV treatment. Considering its high correlation with traits that reassemble a more stem-like cell state (CV treatment and high OFE), and its low correlation with module black, we expected to find in this module pathways that could describe a more stem-like cell/regenerative profile. Pathway analysis revealed that both the Hippo and Wnt pathways were significantly represented in this module for genes known to be involved in stem cells self-renewal (Figure 6 A).

To functionally characterize the role of Wnt signaling in salivary gland stem cells, we assess how pharmacologically inhibition of Wnt pathway in human salivary gland organoids culture influence the ability of salivary gland-derived cells to self-renew. In accordance to what published previously in mouse salivary gland organoids[18], inhibition of the Wnt pathway drastically reduces the self-renewal ability of human salivary gland-derived cells, indicating its fundamental role in the activation and maintenance of salivary gland-derived cells (Supplementary Figure 4A). Notably, treatment with CV induced a "Wnt hyperactivation" phenotype characterize by the upregulation of ligand (*WNT7B*), receptor (*LGR6*), transcription factor of the Wnt pathway (*TCF7*, *LEF1*) and target gene (*AXIN2*). Among the Wnt target gene, *PPARδ*, a peroxisome proliferator activated receptor, nutrient sensor, as well as transcriptional regulator of enzymes involved in lipid metabolism and fatty acid oxidation (FAO), was upregulated in CV treated salivary gland-derived organoids (Figure 6B). We next investigated whether overexpression of *PPARδ,* and potentially stimulation of FAO, in freshly isolated human salivary gland-derived cells, would increase their OFE ability in the absence of CV treatment (Figure 6C). The higher OFE, and total cell number, observed in *PPARδ*-mCherry+ cells compared to their negative counterpart (*PPARδ*-mCherry-) could indicate a role of the lipid metabolism pathway in determining salivary-gland derived cell fate decision (Figure 6 D and E).

When looking at the genes enriched within the Hippo pathway, we saw that CV treatment led to an increased expression of YAP target genes such as *WWC1, PPP2R2B and PP2R2D*, indicating that CV treatment promotes a YAP active state, similar to what has been recently described upon RXRi treatment in the intestinal organoid regenerative signature (Lukonin I et al 2020). Interestingly, module IndianRed3 showed an enrichment for genes involved in the regulation of pluripotent stem cells (P value = 2.7E-2). Interestingly, *PAX6* expression in human-derived salivary gland organoids was similar to the Pax6 expression measured in E18 and 6-week-old mouse submandibular glands [27]. *JARIG2*, a polycomb repressive complex2 (*PRC2*) recruiting protein, has been found to be abundantly expressed in embryonic stem cells as hub component of the pluripotency network[28] involved in the priming of embryonic stem

cells necessary for later stages of development [29]. Together, this data suggests that the different biological processes identified within the IndianRed3 module are integrated to induce and maintain a proliferative, non-differentiated phenotype of salivary gland-derived organoid cells.

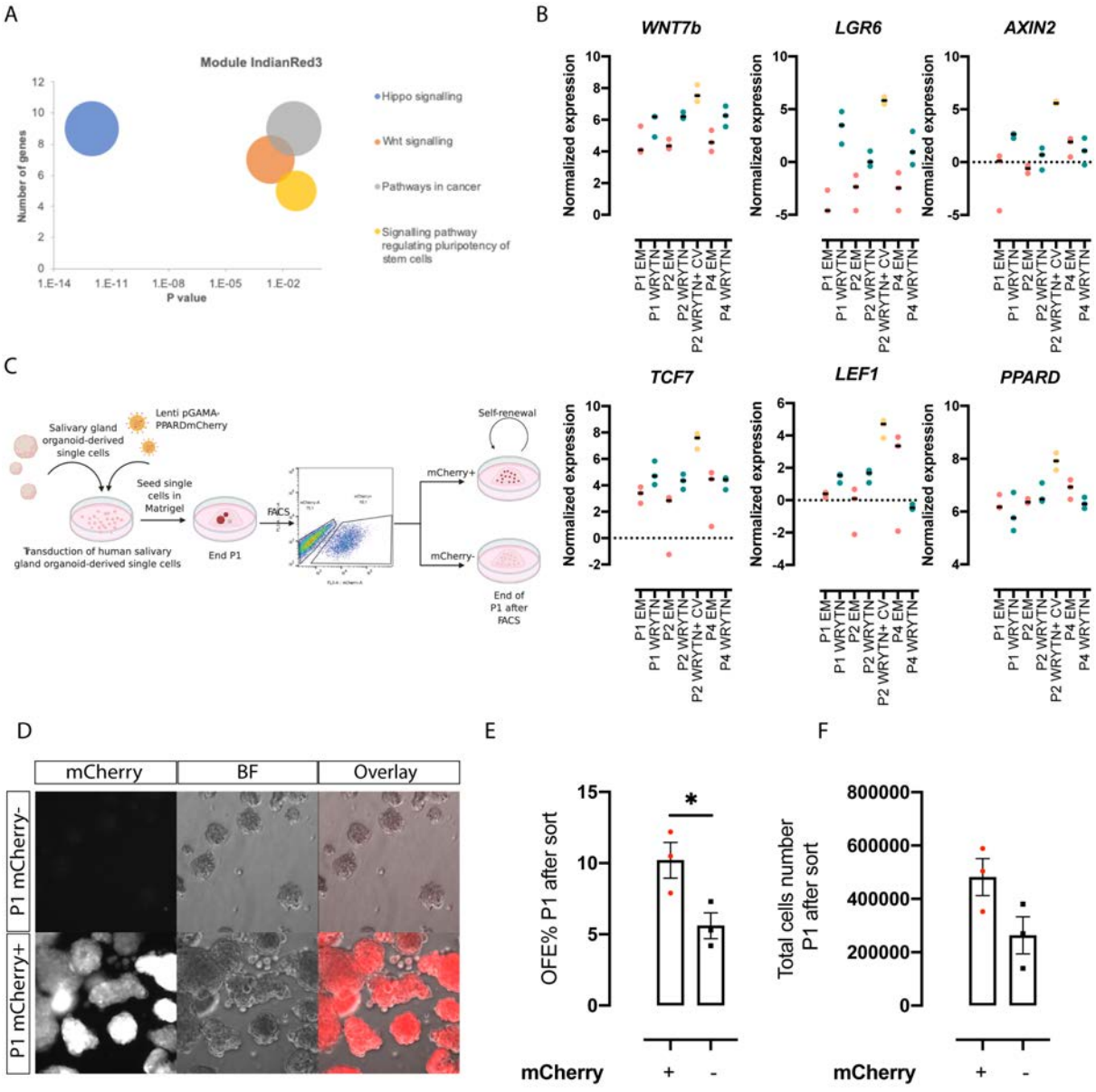

Figure 6: Module IndianRed3 is directly affected by CV treatment and identifies a proliferative, non-differentiated phenotype of salivary gland organoid-derived cell. A) Bubble chart representation of the significant pathways obtained by DAVID pathway analysis on MEIndianRed3 driver genes (module membership >0,6). Each colour represents a different pathway. The size of the bubble represents the significance of the pathway (P<0.05) and the number of genes enriched in the pathway. **B)** Normalized gene expression of the genes enriched in the Hippo and Wnt pathway throughout the different culture passages. Each dot represents a single patient. **C)** Workflow of the lentiviral overexpression experimental procedure used to validate the role of *PPARδ* in human salivary gland-derived cells self-renewal. **D)** Representative images and **(E)** quantification of secondary organoids and **(F)** total number of cells derived from *PPARδ* overexpression cells (mCherry+) compared to control (mCherry-

). Each dot represents a single patient. Data are represented as the mean ± SEM. One-way ANOVA (E)(F). *p<0.05.

A potential transient amplifying (TA) cell signature is associated with long-term self-renewal of human salivary gland-derived cells

We further interrogated the renewal of salivary gland-derived organoids by examining module Sienna4, which based on the Bayesian network analysis was directly linked to the OFE trait. Considering that no enrichment treatment was applied to these cells, this module contains genes that might be responsible for the ability of human salivary gland-derived cells to form organoids over time in culture. Interestingly, the focal adhesion pathway and the hippo pathway were the two pathways highly enriched within the driver genes of module Sienna4, indicating a potential role and interconnection of these pathways in long term maintenance of human salivary gland-derived organoids (Figure 7A). Focal adhesions (FAs) are specialized multiprotein assemblies located within the cells that strongly interact with the extracellular matrix (ECM) and function as dynamic mechanosensor and as upstream regulator of signaling pathways, including the Hippo pathway, in response to environmental changes [30,31].The progressive increase in gene expression of integrin α3 (*ITGα3*), tyrosine kinase *SRC* and the small GTPases *RAC2*, both mediator of FAK signaling, within passages, and their downregulation at P4 EM compared to P4 WRYTN (Figure 7B), could highlight a role of the axis *ITG3-SRC-RAC* in maintaining the ability to form organoids, perhaps via promoting Yap activation in a Lats1/2 independent manner as described in the transient amplifying cells of the mouse incisor[32]. By mining the Human Protein atlas dataset, we found that both *SRC* and *RAC2* were expressed in the basal layer cells of the main striated ducts (Figure 7C). This pattern might suggest that Yap activity via *ITG3-SRC-RAC2* could be stimulated in the basal layer of these cells.

To test if our analysis could enable the identification of potential stem/progenitor cell markers within the salivary gland, we choose *ELOVLI1* (Fatty Acid Elongase 1) which was the first gene within module Sienna4 with high module membership (module membership = 0,853) known to be expressed in salivary gland (Figure 7D). *ELOVL1* is also known to be highly expressed in skin, stomach, lung and kidney and it has been shown to play a central role in the organogenesis of organ depending on high lipid metabolism. Deletion of Elovl1 was found to reduce the expression of genes necessary for bladder epithelium development in zebrafish such as Sox2 and Hb9[33]. Additionally, in mice *ELOVL1* knock out is responsible for the evaporative dry eye phenotype characteristic of aged-induced corneal damage[34]. Here to establish if *ELOVLI1* is expressed in stem/progenitor cells within the salivary gland we first assess its localization within the adult submandibular gland tissue. *ELOVLI1* expression was found mainly in the ductal compartment indicating that the ductal cells might relay on fatty

acid/lipid metabolism (Figure 7E, inset 1 and 2, and F). To test if *ELOVL1* could play a functional role in salivary gland regeneration, we used our organoid culture system as a regenerative model to assess the self-renewal potential of *ELOVL1* overexpressing cells (Figure 7G). We transduced salivary gland-derived cells at the end of P1 with a lentiviral vector encoding for *ELOVL1*-t2A-mCherry and sort for mCherry+ cells one week after transduction. Sorted mCherry+ cells seeded in Matrigel showed higher OFE compared to mCherry- cells indicating, in accordance with the PPARδ finding, that increased fatty acid metabolism can promote the self-renewal of salivary gland-derived cells (Figure 7I and L).

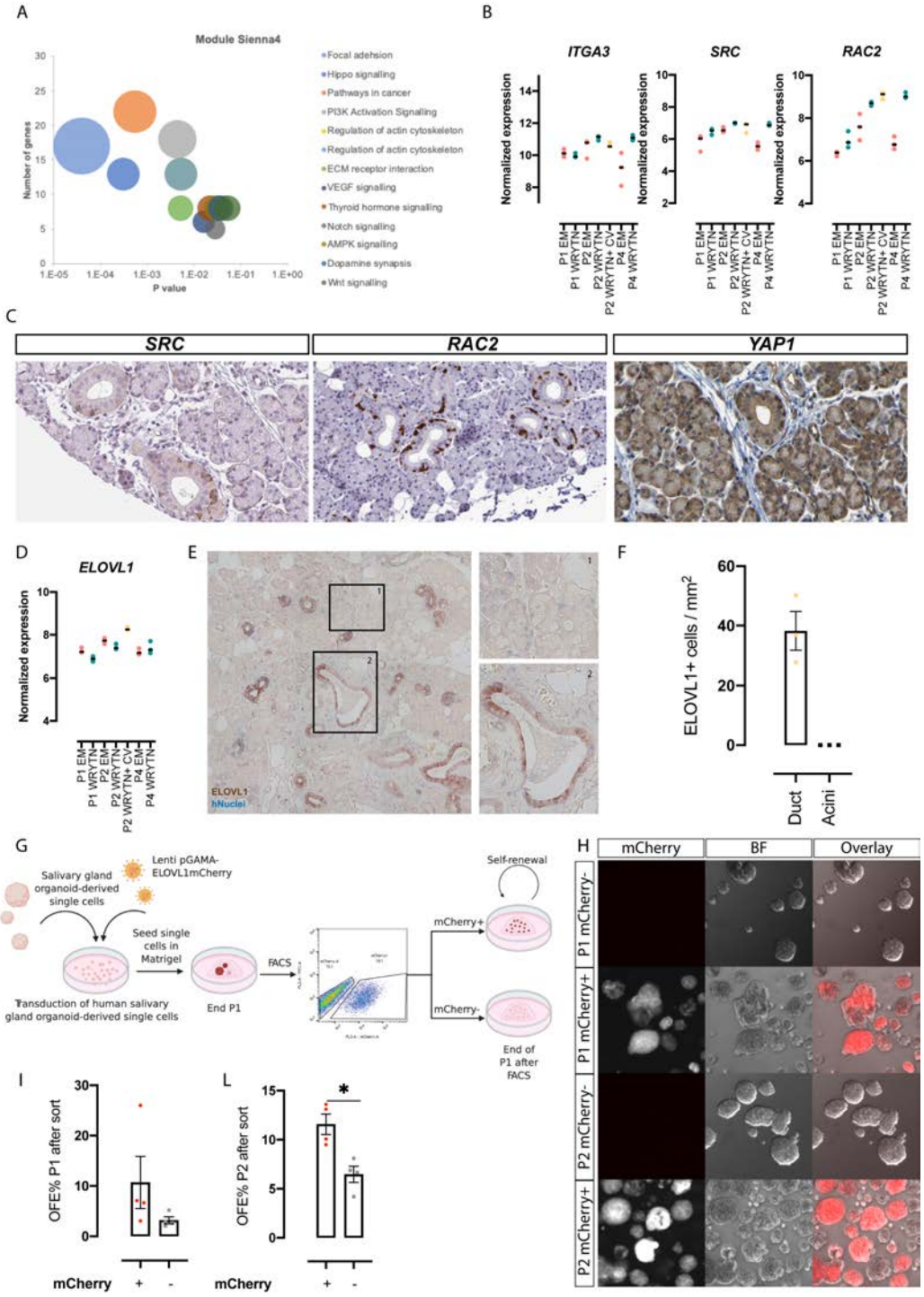

Figure 7: Module Sienna4 genes transcription profile identified an enrichment for potential transient amplifying cells. A) Bubble chart representation of the significant pathways obtained by DAVID pathway analysis on MESienna4 driver genes (module membership >0,6). Each colour represents a different pathway. The size of the bubble represents the significance of the pathway (P<0.05) and the number of genes enriched in the pathway. **B)** Normalized gene expression of the genes enriched in the Focal adhesion pathway. Each dot represents a single patient. **(C)** IHC staining of SCR, Rac2 and YAP1 in human submandibular gland biopsies, showing expression of these protein in the basal layer of the main excretory duct. **D)** Normalized gene expression ELOVL1. Each dot represents a single patient. **E)** ELOVL1 staining in human submandibular gland tissue (Brown) counterstained with hNuclei staining (Blue). Inset 1 shows a region with a main excretory duct positive for ELOVL1. Inset 2 shows acinar cells negative for ELOVL1. **(F)** Quantification of ELOVL1 positive cells per mm^2 of tissue. Patient tissue

biopsies analyzed n=3. **(G)** Workflow of the lentiviral overexpression experimental procedure used to validate the role of *ELOVL1* in human salivary-gland derived cells self-renewal. **H)** Representative images and **(I)** quantification of secondary and **(J)** tertiary organoids derived from ELOVL1 overexpressed cell (mCherry+) compared to control (mCherry-). Data are represented as the mean ± SEM. One-way ANOVA. *p<0.05.

DISCUSSION

In this study we used a gene co-expression analysis approach to identify biological processes and specific genes responsible for the self-renewal and differentiation of human salivary gland-derived cells. The key feature of our approach is the identification of direct molecular-phenotypic stem cell trait relationships which increase the chances of discovering salivary gland specific stem cell associated features. We applied the network analysis to a set of different human-derived salivary gland organoid culture conditions aimed at enriching either for stem cells or for functional secretory salivary gland cells. The framework adopted and our data were able to identify different sets of co-expressed genes that describe biological processes that directly relate to long-term self-renewal and stem cell pluripotency, well separated from those set of genes that instead describe a secretory salivary gland function.

While salivary gland-derived cells have been shown to hold therapeutic potential to treat the irradiation-induced hyposalivation phenotype, little is known about the underlying mechanisms that control their regenerative potential: whether through a direct contribution to replenishing cell loss or due to paracrine effects of the transplanted cells on the surrounding damaged tissue[8,15,35]. The major bottle neck of exploring salivary gland epithelial intrinsic processes *in vivo*, is the slow turnover of the tissue, the current lack of a stem cell marker (or markers) that would allow for the enrichment of a specific cell population by FACS, as well as the emerging view that more than “professional” stem cells, plasticity mechanisms are responsible for the regenerative potential of the glands[15,16] (Rocchi et al 2020, npj Accepted). The recent progress in the organoid field has allowed the growth of slow turnover tissue-derived epithelial cells (mostly non-dividing), including the salivary gland [17,18], by providing niche signaling that coaxes them into an active regenerative state. The possibility to expand salivary gland organoid cultures in a defined medium that allows maintenance of the stem/progenitor pool, as well as differentiation into all salivary gland lineages[18], makes them a perfect tool to tackle this bottle neck. The large quantity of cells derived from organoid cultures allow for the enrichment of rare cell types thereby potentially increasing the resolution of the data generated. Furthermore, the regeneration process mimicked by the development of organoids[36] could enable the investigation of tissue-specific mechanisms that may control tissue renewal, regulation of stem/progenitor cells and cell fate specification.

Isolated salivary gland cells can be induced to form organoids when cultured in Matrigel®. Similar to mouse salivary gland-derived cells[18], in this study, we have shown that human-

derived salivary gland cells are Wnt-responsive and could be stimulated to proliferate, to a certain extent, and form organoids upon exogenous Wnt stimulation. However, in contrast to mouse salivary gland-derived cells, the limited expansion potential of human salivary gland-derived cells, observed under Wnt stimulation, suggested that other pathways might be involved and required for their expansion. Now we have shown that, similar to human liver culture[37], the addition of Tgfβ inhibitor and Noggin to the culture medium allowed the expansion and long term-maintenance of human salivary gland-derived organoids. While the heterogeneous cellular composition of organoids derived from a single cell constitutes one of their major strengths, this same quality could represent a challenge when investigating gene co-expression regulation. Indeed, many variables are likely to influence the detection of a cell type-specific molecular signature from transcriptomic data. The representation of a given cell type and its quantitative relationships with other cell types within the sample, the number of unique genes expressed within this population, the sensitivity of the platform used, the number of samples and even the bioinformatic approaches used to identify gene-expression modules are all parameters which can influence cell type-specific transcriptomic signatures[38].

Here, by adding small molecules to the optimized expansion medium (CHIR99090 and valproic acid), we were able to enrich for specific cellular states, e.g. stem/progenitor cells-like state, and overcome the limitations imposed by the lack of a cellular surface marker in enriching for a specific cell type. This strategy, combined with a bulk-RNA sequencing strategy and a molecular network framework (WGCNA), allowed us to obtain an unbiased, wide overview of the complexity of the regulatory network responsible for organoid renewal and differentiation. Indeed, we show that the early inhibition, at a single cell stage, of GSK3B and the induction of chromatin remodeling, using the histone deacetylase inhibitor valproic acid, seems to promote a Wnt hyperactive transcription profile and a switch to a more pluripotent state. Under these conditions organoid-derived cells display a significant increase in proliferation, while at the same time they lose the ability to acquire a mature differentiation phenotype and salivary gland specification. This may indicate a more “regenerative” profile similar to what has been recently described for intestinal derived organoids[36,39]. While further investigation will be needed to confirm a metabolic role in self-renewal ability of salivary gland-derived cells, the high expression of Pparδ could suggest the activation of a Pparδ-driven FAO program upon CV treatment. Activation of FAO could be responsible for the increased fraction of proliferating cells able to give rise to organoids, as well as for the possible “rejuvenation” of aged salivary gland organoid-derived cells[40].

While manipulation of medium composition is a fundamental requirement to study and to understand the *in vitro* biological processes behind organoid formation, likewise, is the manipulation of the ECM in which the cells are cultured. Our gene co-expression analysis

provided evidence that the ability to give rise to organoids and the maintenance of salivary gland organoid culture could be dependent on integrin expression levels. Interestingly, the integrin-driven Yap activation program suggested here could enable the transition of stem-like cells (P1) to a higher proliferative TA-like state (P2-P4). These results could be used to identify critical gel components in organoid formation that could be used to create a well-defined, dynamic, synthetic matrix potentially suitable for GMP-compliant procedure.

Despite CV treatment seeming to enrich for a more pluripotent-like phenotype and increased passaging for a TA-like phenotype, these organoids seem to lose the salivary gland specification that characterizes the P1 organoids. The progressive decline of the acinar development profile within passages indicates that differently from mouse-derived salivary gland organoid culture [18], human-derived salivary gland culture conditions are not yet "permissive/tuned" to maintain long-term the heterogeneity and self-organizing potential that define mouse-derived salivary gland organoids, as well as intestinal organoids[41,42]. This could be due the fact that the enrichment provided by current culture conditions hinders human-derived salivary gland organoids to undergo symmetry breaking (Serra et al; 2018), while maintaining a more "hyperactivation-like state" or a more "regenerative-like state" [39]. While the bulk RNA sequencing approach represents more a screen-shot of the organoids' transcriptomic profile at the end of the culture, organoid single cell RNA sequencing could enable the identification of how the transcriptomic profile of single cells changes under different conditions and shed light on possible symmetry breaking mechanisms in salivary gland organoids. From the co-expression gene analysis presented here, P1 organoids are the only ones that retain a secretory acinar transcription profile, indicating that these organoids better resemble the complex multicellular structure of the salivary gland tissue of origin. Therefore, they are the ones that can potentially recapitulate first the regeneration of the epithelium and subsequently the re-establishment of tissue homeostasis[36,39,42]. Single cell sequencing analysis of these P1 human salivary gland-derived organoids could potentially allow the discovery of the equivalent of the intestinal Paneth cells, responsible for creating the niche environment and the correct formation of intestinal crypt in intestinal organoids, and shed light on the dynamics of salivary gland organoid development. The understanding of single cell trajectories, an integrated multiomic approach combined with time course experiments and genetics-based perturbation (e.g CRISPR-CAS) could allow further elucidation of cell-fate switches in salivary gland organoids. These switches could then be used to guarantee a long-term expansion of complex multicellular organoids that retain salivary gland specification.

Our study represents the first transcriptomic analysis of human-derived salivary gland organoids and a rich resource of information for the salivary gland community. The information gained by the co-expression gene analysis will open up new possibilities for the use of salivary

gland organoids, both in terms of tissue regeneration model as well as a model for the understanding the underlying biological pathways involved in the balance between tissue homeostasis and regeneration.

MATERIAL AND METHODS

Patients

Human non-malignant submandibular gland tissues were obtained from donors after informed consent and Institutional Review Board (IRB) approval during an elective head and neck dissection procedure for the removal of squamous cell carcinoma of the oral cavity at the University Medical Centre Groningen (UMCG) and Medical Centre Leuwaarden (MCL).

Isolation of human submandibular gland derived cells

Human submandibular gland biopsies were collected in the operating room and transferred to the lab in a 50 mL falcon tube containing HBSS 1% BSA on ice. The biopsy was weighted in a sterile petri dish and minced into small pieces using a sterile disposable scalpel. The minced tissue was transfer to GentleMACS C tubes and digested in Hank's Balanced Salt Solution (HBSS) containing 1% bovine serum albumin (BSA; Invitrogen) and supplemented with collagenase type II (0,63mg/mL; Gibco), hyaluronidase (0,5 mg/mL, Sigma-Aldrich) and $CaCl_2$ (6.25mM; Sigma-Aldrich).To obtain optimal digestion 20 mg of tissue was processed per 1 mL of digestion buffer volume, with a maximum of 100 mg of tissue per tube. Two rounds of mechanical digestion were performed using GentleMACS tissue dissociator. In between mechanical digestions, the tubes were incubated in a shaking water bath for 30 minutes at 37°C. At the end of the digestion, cells were collected by centrifugation at 400 G for 5 minutes, the cell pellets washed thoroughly with HBSS 1%BSA, filtered through a 100 μm cell strainers (BD Biosciences) and spun at 400G for 5 minutes. The pellet was resuspended in Dulbecco's modified Eagle's medium: F12 (DMEM F12) containing Pen/Strep antibiotics (Invitrogen), Glutamax, 20 ng/mL epidermal growth factor (EGF; Sigma Aldrich), 20 ng/mL fibroblast growth factor-2 (Sigma- Aldrich), N2 (Invitrogen), 10 μg/mL insulin (Sigma-Aldrich) and 1 μM dexamethasone (Sigma-Aldrich).and cell number counted with the use of Scepter Cell Counter. Only cells within t range size between 6,126 μm and 8,467 μm were taken in consideration. The cell clumps obtained were seeded at a density of $4x10^4$ cells per well in a 6-well plate and incubate at 37°C and 5% CO_2 for 3 days as floating primary culture.

Self-renewal assay of human salivary gland derived cells

Three days-old primary culture were harvested and dispersed to single cells suspension using 0,05% trypsin EDTA (Invitrogen). Single cells were counted and resuspended in culture media at a final concentration of or $0,8x10^6$ cells per mL. 25 μL of cell suspension was mix on ice with 50 μL of ice cold Matrigel and the 75 μL gel pipetted in the middle of a 12-well plate. Following polymerization of the Matrigel ®, 1mL of culture media was added. The culture media used in this study are described as follow. Enriched media (EM): EM; DMEM/F12,

pen/strep [1x; Invitrogen], glutamax [1x; Invitrogen], N2 [1x; Gibco], EGF [20ng/mL; Sigma Aldrich], FGF2 [20ng/nL;sigma Aldrich], insulin [10μg/mL;Sigma Aldrich], dexamethasone [1μM; Sigma Aldrich], Y27632 [10μM; Sigma Aldrich]. Wnt enriched media (WRY): DMEM/F12, pen/strep [1x; Invitrogen], glutamax [1x; Invitrogen], N2 [1x; Gibco], EGF [20ng/mL; Sigma Aldrich], FGF2 [20ng/nL;sigma Aldrich], insulin [10μg/mL;Sigma Aldrich], dexamethasone [1μM; Sigma Aldrich], Y27632 [10μM; Sigma Aldrich], 10% R-spondin1 conditioned medium and 50 % Wnt3a conditioned media. WRYTN: DMEM/F12, pen/strep [1x; Invitrogen], glutamax [1x; Invitrogen], N2 [1x; Gibco], EGF [20ng/mL; Sigma Aldrich], FGF2 [20ng/nL;sigma Aldrich], insulin [10μg/mL;Sigma Aldrich], dexamethasone [1μM; Sigma Aldrich], noggin[50ng/mL; Preprotech-Bioconnect], A8301[1μM Tocris], Y27632 [10μM; Sigma Aldrich], 10% R-spondin1 conditioned medium and 50 % Wnt3a conditioned media. One week after seeding (end of the passage), the media was replaced with Dispase enzyme (1 mg/mL in DEMEM F12 at 37°C for 30-45 minutes) to dissolve the gels. All the organoids released from the dissolved gels were processed to single cells using 0,05% trypsin-EDTA treatment to form single cell suspension. Organoids and cell number at the end of the passage were noted and the secondary organoid derived single cells re-seeded in Matrigel to start a new passage. Number of organoids and single cells at the end of each passage were used to calculate Organoid Formation Efficiency percentage (OFE%) and Population Doubling as follows:

$$Organoid\ Formation\ Efficiency\ (OFE\%) = \frac{Number\ of\ Organoid\ harvested\ at\ the\ end\ of\ the\ pasaage}{Number\ of\ single\ cells\ seeded\ at\ the\ beginning\ of\ the\ passage}\ x\ 100$$

$$Population\ Doubling = \frac{\ln(harvestes\ cells/seeded\ cells)}{ln2}$$

Treatment of human salivary gland derived organoid with CHIR99201 and valproic acid

For comparison of different culture conditions, small molecule as CHIR99021 [3μM] and valproic acid [1μM] were added to the WRYTN media. The cells were kept in culture for 7 days and the media was changed every two days. At the end of the passage the number of organoids and cells number were determined as described above. Organoid-derived single cells were re-seeded in the next passage at a density of $0{,}8x10^6$ cells per mL and culture in absence of CHIR99201 and valproic acid (washout experiment).

Differentiation assay

Human salivary gland-derived organoids were kept in culture for 7 days in WRYTN expansion media in presence or absence of CHIR99201 and valproic acid. At the end of the passage, the media was harvested and ice-cold PBS 1%BSA was added to the well to dissolve the

Matrigel® and release organoids. Organoids were harvested and spun at 400G for 5 minutes. The pellet was re-suspended in 1mL differentiation media and kept on ice. Organoids were counted and seeded at a final density of 20-30 organoids per 75 μL of gel (25 μL media + 50 μL Matrigel®) in a Matrigel ® pre-coated 96 well plate. Following polymerization of the gel at 37°C, 150 μL of differentiation media with/or without CHIR99201 and valproic acid was added on top of the gel. Organoid were harvested after 6 days for RNA sequencing analysis and after 30 days for immunofluorescence and immunohistochemistry analysis of salivary gland specific proteins. Differentiation media is described as follow: DMEM/F12, pen/strep [1x; Invitrogen], glutamax [1x; Invitrogen], HGF (Preprotech), FGF-10 (Preprotech), Heparin salt (Stem Cell Technology), DAPT (Sigma), FCS (Greiner).

Immunofluorescence and immunohistochemistry staining of human salivary gland-derived organoid.

Organoids cultured in Matrigel ® were harvested, washed and fixed by using 4%PFA for 10-30 minutes at room temperature. For whole mount staining Samples were wash with 0,2% BSA PBS and permeabilized with a blocking solution (0,5% triton, 1% BSA in PBS) for 1 hour 30 minutes at room temperature with gentle shaking. Sample were incubated with primary antibody staining in blocking buffer at 4 °C for 24-48 h. Secondary antibody (1:250) and DAPI staining were performed in 0,1%BSA PBS at room temperature over night with gentle shaking. Sample were thoroughly washed with 0,1% BSA PBS and mount on an object glass for imaging Images were acquired by using Leica SP8 confocal microscope. For AQP5, Amylase immunofluorescence staining on differentiated organoid, 4 μm paraffine section were deparaffinize and incubated at 4 °C overnight, after citrate-mediated antigen retrieval, with primary antibodies as follow: anti-Aqp5 (1:200, Abcam), anti-α amylase (1:200, Sigma). Section were washed and incubated with secondary antibody for 2h at room temperature in the dark. DAPI was used as nuclei counterstaining. Imaging were acquired using Leica DM6000 B and processed using Image J software. For immunohistochemistry detection of Mucin, paraffine section were processed as described above and incubated in Alcian Blue solution (Alcian blue 8GX Sigma, A5268) for 30 minutes at room temperature. Nuclei were visualized by using nuclear fast red counterstaining for 5 minutes at room temperature. Section were washed, rehydrate and mount using Eukit (Sigma).

Lentiviral production and lentiviral transduction of human salivary gland-derived cells.

HEK293T cells were plated in poly-L-lysin coated 10 cm dish at a density of $1,5x10^6$ and cultured in DMEM supplemented with 10% FBS, Pen/Strep [1x; Invitrogen], Glutamax [1x; Invitrogen] and incubated ON at 37°C and 5% CO_2. On the next day cells were transfected

with 3 μg of p-GAMA PPARδ, p-GAMA ELOVL1 (AddGene) [30] or empty p-GAMA 3 μg of the packaging plasmid PAX2, 0,7 μg of envelope plasmid VSV-G and 40 μL of PEI (1 μg/mL) as previously described [40]. On the next day medium was changed to DMEM F12. Two days after transfection the viruses were collected, filtered through a sterile syringe filter with a 0,45 μm pore size and hydrophilic PVDF membrane and frozen in 250 μL aliquots at -80 °C. We have tittered the virus-containing supernatant by transduction of mCherry gene. Viruses were always in the range of $5,0x10^6$ – $7,0x10^6$ transduction unit (TU)/mL.

At end of the passage culture media was removed and Dispase (Gibco) was added. After incubation at 37°C for 30 minutes, organoid were harvested, washed and dissociated to single cells by using 0.05% trypsin-EDTA (Invitrogen). Human salivary gland organoid-derived single cells were counted and resuspended in WRYTN media to a final concentration of $2.5x10^6$ cells per mL. For each 100 μL of cell suspension 250 μL of viral supernatant and polybrene (6 μg/mL) was added. The mixture was divided in 350 μL aliquots in a 24-well plate and incubated ON at 37°C and 5% CO_2. The day after transduction single cells were counted to adjust for dead cells, resuspended in media to a final concentration of $0,8x10^6$ cells per mL and seeded in Matrigel into 12-well plate. The cells were cultured for 7 to 10 days in WRYTN media at 37°C and 5% CO_2.

Flow Activate Cell Sorted (FACS) analysis

At day 7 cell culture media was removed Matrigel was dissolved with the use of Dispase (1 mg/mL; Gibco) and organoids dispersed to single cells with the use of 0.05% trypsin-EDTA. Cells were washed with 0.2% BSA in PBS and resuspended in 0.2% BSA with the viability dye (DAPI) in PBS. PPARδ and ELOVL1 overexpressing cells were isolated by fluorescence-activated cell sorting for mCherry-positive cells, seeded in Matrigel and cultured in EM. Organoid forming efficiency and cell number were assessed as described above.

Immunoblot

To monitor endogenous gene responses, mouse and human organoids were harvested and centrifuged pellets homogenized by sonication in 2x Laemnli buffer. Protein concentration of the lysates was determined using Bradford quantification method. Homogenates were then boiled at 99°C for 5 minutes and equal protein amounts were separated with 10 or 12% polyacrylamide gels and transfered to PVDF membranes using Trans Blot Turbo System (Bio-Rad). The membranes were blocked in 5% BSA in PBS-Teween-20 and incubated 1 h at RT. Incubation with primary antibodies was done ON at 4°C following by incubation with HRP-conjugated secondary antibodies. Membranes were developed using ECL reagent (Thermo Fisher Scientific) and the signal was detected using ChemiDoc imager (Biorad). Densiometric

analysis of western blots at non-saturated exposure were performed using Image J software and the values normalized against the one of GAPDH loading control. For immunoblots, the following primary antibodies at the indicated dilutions were used: rabbit anti-ELOVL1; mouse anti-GAPDH (Fitzgerald) 1:10000

RNA isolation and RNA sequencing data generation

Human salivary gland-derive organoids were harvested and stored in RNA later. Total RNA was isolated form individual samples was performed using Quigen RNeasy micro kit according to the manufacture instruction. RNA quality and quantity were assessed using Bioanalyzer assay and only sample with a concentration of > 10ng and RNA integrity scores (RIN) of > 8.5 were used to generate the libraries. NEXTflex™ Poly (A) Beads kit was used to isolate pure and intact messenger RNA (mRNA). RNA sequencing library were prepared using NETflex™ Rapid Directional qRNA-Seq ™ kit accordingly to manufacturer's protocol. FastQC (version 0.11.5) was utilized to perform quality control checks on the raw sequence data. Reads were aligned to the human genome using Spliced Transcripts Alignment to a Reference (STAR) (version 2.5.3a). Aligned reads were normalized excluding low abundance genes. Principal component analysis was performed on the 30 samples in order to detect extreme outlier.

Weighted gene co-expression network analysis (WGCNA)

Gene co-expression analysis was performed on the normalized RNA-Seq expression data (Log2 cpm), using the R package WGCNA [43]. All 30 samples were included in the analysis. Genes were clustered into modules by using the average linkage hierarchical algorithm [43].All cluster consisting of at least 30 genes were identified and summarized by their module eigengene[24]. Highly similar modules were merged together is their Pearson correlation coefficient exceed 0.25. At the end of the analysis 59 co-expression modules were identified. To identify key driver genes within the modules we determined the strength of module membership for each gene in the module. Module membership is determined by calculating the Pearson correlation of the expression profile of every gene in the module with the module eigengene. Genes that have had module membership of > 0.6 were genes that were considered highly connected within the module[24] (https://horvath.genetics.ucla.edu/html/CoexpressionNetwork/Rpackages/WGCNA/Tutorials/).

To identify possible stem cell related modules, we investigated the relationship of each module with known stem cells related traits: ability of self-renew and ability to differentiate. We performed Pearson correlation between the module eigengene of each module and the sample phenotypic trait (OFE, CV and P1). Modules that have a high correlation (value -1 to 1) and high significance of the correlation (P<0,05) with the module eigengene were selected.

Bayesian network structure learning to estimate the module-trait network

A Bayesian network are graphical models where nodes represent random variables and arrows represent probabilistic dependencies between them[25]. We create the Bayesian network using bnlearn package (version 4.2) using the hill climbing learning structure(https://www.bnlearn.com) to predict the directed acyclic graph (DAG) that describe the dependencies and relationship between two types of variable: modules stem cell phenotypic traits.

Pathway analysis

GO term enrichment analysis of modules driver genes was performed using Database for Annotation, Visualization and Integrated Discovery Functional Annotation Tool (DAVID v6.770) (www.david-d.ncifcrf.gov). Bubble plots representing most represented pathway were created with Excel based on the significance of the pathway given by DAVID and the number of gene enriched per pathway.

Statistical Analysis

All statistical analyses in this study were performed using GraphPad Prism8 software (GraphPad, La Jolla, CA, USA). The number of mice, patients or individual organoids analyzed (n), presented error bars (SEM), statistical analysis and p values are all stated in each figure or figure legend.

REFERENCES

1 Emmerson, E. & Knox, S. M. Salivary gland stem cells: A review of development, regeneration and cancer. *Genesis* **56**, e23211, doi:10.1002/dvg.23211 (2018).

2 Pringle, S., Van Os, R. & Coppes, R. P. Concise review: Adult salivary gland stem cells and a potential therapy for xerostomia. *Stem Cells* **31**, 613-619, doi:10.1002/stem.1327 (2013).

3 Tsai, W. L., Huang, T. L., Liao, K. C., Chuang, H. C., Lin, Y. T., Lee, T. F. *et al.* Impact of late toxicities on quality of life for survivors of nasopharyngeal carcinoma. *BMC Cancer* **14**, 856, doi:10.1186/1471-2407-14-856 (2014).

4 Rocchi, C. & Emmerson, E. Mouth-Watering Results: Clinical Need, Current Approaches, and Future Directions for Salivary Gland Regeneration. *Trends Mol Med* **26**, 649-669, doi:10.1016/j.molmed.2020.03.009 (2020).

5 Vissink, A., Jansma, J., Spijkervet, F. K., Burlage, F. R. & Coppes, R. P. Oral sequelae of head and neck radiotherapy. *Crit Rev Oral Biol Med* **14**, 199-212, doi:10.1177/154411130301400305 (2003).

6 Vissink, A., Mitchell, J. B., Baum, B. J., Limesand, K. H., Jensen, S. B., Fox, P. C. *et al.* Clinical management of salivary gland hypofunction and xerostomia in head-and-neck cancer patients: successes and barriers. *Int J Radiat Oncol Biol Phys* **78**, 983-991, doi:10.1016/j.ijrobp.2010.06.052 (2010).

7 Lombaert, I. M., Brunsting, J. F., Wierenga, P. K., Faber, H., Stokman, M. A., Kok, T. *et al.* Rescue of salivary gland function after stem cell transplantation in irradiated glands. *PLoS One* **3**, e2063, doi:10.1371/journal.pone.0002063 (2008).

8 Pringle, S., Maimets, M., van der Zwaag, M., Stokman, M. A., van Gosliga, D., Zwart, E. *et al.* Human Salivary Gland Stem Cells Functionally Restore Radiation Damaged Salivary Glands. *Stem Cells* **34**, 640-652, doi:10.1002/stem.2278 (2016).

9 Emmerson, E., May, A. J., Berthoin, L., Cruz-Pacheco, N., Nathan, S., Mattingly, A. J. *et al.* Salivary glands regenerate after radiation injury through SOX2-mediated secretory cell replacement. *EMBO Mol Med* **10**, doi:10.15252/emmm.201708051 (2018).

10 Peng, X., Wu, Y., Brouwer, U., van Vliet, T., Wang, B., Demaria, M. *et al.* Cellular senescence contributes to radiation-induced hyposalivation by affecting the stem/progenitor cell niche. *Cell Death Dis* **11**, 854, doi:10.1038/s41419-020-03074-9 (2020).

11 Baum, B. J., Alevizos, I., Zheng, C., Cotrim, A. P., Liu, S., McCullagh, L. *et al.* Early responses to adenoviral-mediated transfer of the aquaporin-1 cDNA for radiation-induced salivary hypofunction. *Proc Natl Acad Sci U S A* **109**, 19403-19407, doi:10.1073/pnas.1210662109 (2012).

12 Lombaert, I. M. A., Patel, V. N., Jones, C. E., Villier, D. C., Canada, A. E., Moore, M. R. *et al.* CERE-120 Prevents Irradiation-Induced Hypofunction and Restores Immune Homeostasis in Porcine Salivary Glands. *Mol Ther Methods Clin Dev* **18**, 839-855, doi:10.1016/j.omtm.2020.07.016 (2020).

13 Barker, N., van Es, J. H., Kuipers, J., Kujala, P., van den Born, M., Cozijnsen, M. *et al.* Identification of stem cells in small intestine and colon by marker gene Lgr5. *Nature* **449**, 1003-1007, doi:10.1038/nature06196 (2007).

14 May, A. J., Cruz-Pacheco, N., Emmerson, E., Gaylord, E. A., Seidel, K., Nathan, S. *et al.* Diverse progenitor cells preserve salivary gland ductal architecture after radiation-induced damage. *Development* **145**, doi:10.1242/dev.166363 (2018).

15 Weng, P. L., Aure, M. H., Maruyama, T. & Ovitt, C. E. Limited Regeneration of Adult Salivary Glands after Severe Injury Involves Cellular Plasticity. *Cell Rep* **24**, 1464-1470 e1463, doi:10.1016/j.celrep.2018.07.016 (2018).
16 Ninche, N., Kwak, M. & Ghazizadeh, S. Diverse epithelial cell populations contribute to the regeneration of secretory units in injured salivary glands. *Development* **147**, doi:10.1242/dev.192807 (2020).
17 Nanduri, L. S., Baanstra, M., Faber, H., Rocchi, C., Zwart, E., de Haan, G. *et al.* Purification and ex vivo expansion of fully functional salivary gland stem cells. *Stem Cell Reports* **3**, 957-964, doi:10.1016/j.stemcr.2014.09.015 (2014).
18 Maimets, M., Rocchi, C., Bron, R., Pringle, S., Kuipers, J., Giepmans, B. N. *et al.* Long-Term In Vitro Expansion of Salivary Gland Stem Cells Driven by Wnt Signals. *Stem Cell Reports* **6**, 150-162, doi:10.1016/j.stemcr.2015.11.009 (2016).
19 Zhang, B. & Horvath, S. A general framework for weighted gene co-expression network analysis. *Stat Appl Genet Mol Biol* **4**, Article17, doi:10.2202/1544-6115.1128 (2005).
20 Roccio, M., Hahnewald, S., Perny, M. & Senn, P. Cell cycle reactivation of cochlear progenitor cells in neonatal FUCCI mice by a GSK3 small molecule inhibitor. *Sci Rep* **5**, 17886, doi:10.1038/srep17886 (2015).
21 Roccio, M., Perny, M., Ealy, M., Widmer, H. R., Heller, S. & Senn, P. Molecular characterization and prospective isolation of human fetal cochlear hair cell progenitors. *Nat Commun* **9**, 4027, doi:10.1038/s41467-018-06334-7 (2018).
22 Yin, X., Farin, H. F., van Es, J. H., Clevers, H., Langer, R. & Karp, J. M. Niche-independent high-purity cultures of Lgr5+ intestinal stem cells and their progeny. *Nat Methods* **11**, 106-112, doi:10.1038/nmeth.2737 (2014).
23 McLean, W. J., Yin, X., Lu, L., Lenz, D. R., McLean, D., Langer, R. *et al.* Clonal Expansion of Lgr5-Positive Cells from Mammalian Cochlea and High-Purity Generation of Sensory Hair Cells. *Cell Rep* **18**, 1917-1929, doi:10.1016/j.celrep.2017.01.066 (2017).
24 Horvath, S. & Dong, J. Geometric interpretation of gene coexpression network analysis. *PLoS Comput Biol* **4**, e1000117, doi:10.1371/journal.pcbi.1000117 (2008).
25 Korb, K., Nicholson, A. *Bayesian Artificial Intelligence*. 2nd Edition edn, (CRC Press, 2011).
26 Cawley, A., Golding, S., Goulsbra, A., Hoptroff, M., Kumaran, S. & Marriott, R. Microbiology insights into boosting salivary defences through the use of enzymes and proteins. *J Dent* **80 Suppl 1**, S19-S25, doi:10.1016/j.jdent.2018.10.010 (2019).
27 Tanaka, J., Ogawa, M., Hojo, H., Kawashima, Y., Mabuchi, Y., Hata, K. *et al.* Generation of orthotopically functional salivary gland from embryonic stem cells. *Nat Commun* **9**, 4216, doi:10.1038/s41467-018-06469-7 (2018).
28 Landeira, D., Bagci, H., Malinowski, A. R., Brown, K. E., Soza-Ried, J., Feytout, A. *et al.* Jarid2 Coordinates Nanog Expression and PCP/Wnt Signaling Required for Efficient ESC Differentiation and Early Embryo Development. *Cell Rep* **12**, 573-586, doi:10.1016/j.celrep.2015.06.060 (2015).
29 Sperber, H., Mathieu, J., Wang, Y., Ferreccio, A., Hesson, J., Xu, Z. *et al.* The metabolome regulates the epigenetic landscape during naive-to-primed human embryonic stem cell transition. *Nat Cell Biol* **17**, 1523-1535, doi:10.1038/ncb3264 (2015).

30 Burridge, K. Focal adhesions: a personal perspective on a half century of progress. *FEBS J* **284**, 3355-3361, doi:10.1111/febs.14195 (2017).
31 Kim, N. G. & Gumbiner, B. M. Adhesion to fibronectin regulates Hippo signaling via the FAK-Src-PI3K pathway. *J Cell Biol* **210**, 503-515, doi:10.1083/jcb.201501025 (2015).
32 Hu, J. K., Du, W., Shelton, S. J., Oldham, M. C., DiPersio, C. M. & Klein, O. D. An FAK-YAP-mTOR Signaling Axis Regulates Stem Cell-Based Tissue Renewal in Mice. *Cell Stem Cell* **21**, 91-106 e106, doi:10.1016/j.stem.2017.03.023 (2017).
33 Bhandari, S., Lee, J. N., Kim, Y. I., Nam, I. K., Kim, S. J., Kim, S. J. *et al.* The fatty acid chain elongase, Elovl1, is required for kidney and swim bladder development during zebrafish embryogenesis. *Organogenesis* **12**, 78-93, doi:10.1080/15476278.2016.1172164 (2016).
34 Sassa, T., Tadaki, M., Kiyonari, H. & Kihara, A. Very long-chain tear film lipids produced by fatty acid elongase ELOVL1 prevent dry eye disease in mice. *FASEB J* **32**, 2966-2978, doi:10.1096/fj.201700947R (2018).
35 Zhao, Q., Zhang, L., Hai, B., Wang, J., Baetge, C. L., Deveau, M. A. *et al.* Transient activation of the Hedgehog-Gli pathway rescues radiotherapy-induced dry mouth via recovering salivary gland resident macrophages. *Cancer Res*, doi:10.1158/0008-5472.CAN-20-0503 (2020).
36 Serra, D., Mayr, U., Boni, A., Lukonin, I., Rempfler, M., Challet Meylan, L. *et al.* Self-organization and symmetry breaking in intestinal organoid development. *Nature* **569**, 66-72, doi:10.1038/s41586-019-1146-y (2019).
37 Huch, M., Gehart, H., van Boxtel, R., Hamer, K., Blokzijl, F., Verstegen, M. M. *et al.* Long-term culture of genome-stable bipotent stem cells from adult human liver. *Cell* **160**, 299-312, doi:10.1016/j.cell.2014.11.050 (2015).
38 Oldham, M. C. in *The OMICs: Applications in Neuroscience* (ed Coppola G.) Ch. 6, (Oxford University Press, 2013).
39 Lukonin, I., Serra, D., Challet Meylan, L., Volkmann, K., Baaten, J., Zhao, R. *et al.* Phenotypic landscape of intestinal organoid regeneration. *Nature* **586**, 275-280, doi:10.1038/s41586-020-2776-9 (2020).
40 Mihaylova, M. M., Cheng, C. W., Cao, A. Q., Tripathi, S., Mana, M. D., Bauer-Rowe, K. E. *et al.* Fasting Activates Fatty Acid Oxidation to Enhance Intestinal Stem Cell Function during Homeostasis and Aging. *Cell Stem Cell* **22**, 769-778 e764, doi:10.1016/j.stem.2018.04.001 (2018).
41 Sato, T., Vries, R. G., Snippert, H. J., van de Wetering, M., Barker, N., Stange, D. E. *et al.* Single Lgr5 stem cells build crypt-villus structures in vitro without a mesenchymal niche. *Nature* **459**, 262-265, doi:10.1038/nature07935 (2009).
42 Spence, J. R., Mayhew, C. N., Rankin, S. A., Kuhar, M. F., Vallance, J. E., Tolle, K. *et al.* Directed differentiation of human pluripotent stem cells into intestinal tissue in vitro. *Nature* **470**, 105-109, doi:10.1038/nature09691 (2011).
43 Langfelder, P. & Horvath, S. WGCNA: an R package for weighted correlation network analysis. *BMC Bioinformatics* **9**, 559, doi:10.1186/1471-2105-9-559 (2008).